

Supplement of Hydrol. Earth Syst. Sci., 22, 3933–3950, 2018
<https://doi.org/10.5194/hess-22-3933-2018-supplement>
© Author(s) 2018. This work is distributed under
the Creative Commons Attribution 4.0 License.



Supplement of

Mean and extreme precipitation over European river basins better simulated in a 25 km AGCM

Reinhard Schiemann et al.

Correspondence to: Reinhard Schiemann (r.k.schiemann@reading.ac.uk)

The copyright of individual parts of the supplement might differ from the CC BY 4.0 License.

Contents

List of Tables

S1	River basin names, surface areas in km ² , and HYDRO1k Pfafstetter codes (Verdin and Verdin, 1999).	2
----	--	---

List of Figures

5	S1	Illustration of GEV distribution parameters in a Gumbel diagram. (a) Varying the location parameter μ for constant σ and ξ , (b) varying the scale parameter σ for constant μ and ξ , and (c) varying the shape parameter ξ for constant μ and σ	3
	S2	Estimated GEV parameters for March–May daily basin-average precipitation, (a–c) location parameter μ and (d–f) scale parameter σ , both in mm day ⁻¹ , and for (a,d) observations (E-OBS), (b,e) N96, and (c,f) N512 resolution. Stippling (hatching) shows statistically significant differences between the models and E-OBS (between N512 and N96).	4
10	S3	As Fig. S2 but for autumn (September–November).	5
	S4	Standard deviation of 2–8 day band-pass filtered 500 hPa geopotential height (m) during spring (March–May). (a) ERA-Interim reanalysis, (b,d,g) model (HadGEM3-GA3.0) at resolutions N96, N216, and N512, (c,f,j) model biases with respect to E-OBS, and (e,h,i) differences between model resolutions. Stippling shows statistically significant differences.	6
15	S5	Spring (March–May) mean precipitation. (a) Observations (E-OBS), (b,d,g) model (HadGEM3-GA3.0) at resolutions N96, N216, and N512, (c,f,j) model biases with respect to E-OBS, and (e,h,i) differences between model resolutions. Stippling shows statistically significant differences.	7
20	S6	As Fig. S4 but for summer (June–August).	8
	S7	As Fig. S5 but for summer (June–August).	9
	S8	As Fig. S4 but for autumn (September–November).	10
	S9	As Fig. S5 but for autumn (September–November).	11
25	S10	Spring (March–May) precipitation in mm day ⁻¹ in (a) observations (E-OBS), (b) the N480 model with N96 orography, and (d) the N480 control simulation. (c,f) Model bias with respect to E-OBS, (e) difference between the two model simulations. Stippling shows statistically significant differences.	12
	S11	As Fig. S10 but for summer (June–August).	13
	S12	As Fig. S10 but for autumn (September–November).	14
30	S13	Spring (March–May) ratios of fitted GEV parameters for (a,b) the location parameter μ and for (c,d) the scale parameter σ , between (a,c) the N512 and N96 simulations and between (b,d) the N480 control simulation and the N480 simulation with N96 orography. Hatching shows statistically significant differences.	15
	S14	As Fig. S13 but for summer (June–August).	16
	S15	As Fig. S13 but for autumn (September–November).	17

Table S1. River basin names, surface areas in km², and HYDRO1k Pfafstetter codes (Verdin and Verdin, 1999).

	Basin	Area	Code
1	Danube	781238	8
2	Daugava	86819	936
3	Dnieper	496580	6
4	Dniester	72304	76
5	Don	426521	4
6	Duero	96438	9118
7	Ebro	85323	9116
8	Elbe	139773	916
9	Garonne/Dordogne	79899	91196
10	Guadalquivir	56671	91174
11	Guadiana	65774	91176
12	Kemijoki	55959	9538, 9542
13	Kuban	58159	398
14	Loire	116256	912
15	Mezen	76902	976
16	Neman	97499	934
17	Neva	235441	94
18	Northern Dvina	288979	96
19	Odra	116748	918
20	Onega	65997	958
21	Pechora	289205	98
22	Po	87239	9112
23	Rhine	194228	914
24	Rhone	84878	9114
25	Seine	86223	9132
26	Severn	7818	91372
27	Southern Bug	60246	72
28	Tagus	70091	91178
29	Thames	12424	9136
30	Upper Danube	208085	89
31	Ural	277453	263, 265–269
32	Vistula	194277	92
33	Volga	1446473	27–29

References

Verdin, K. and Verdin, J.: A topological system for delineation and codification of the Earth's river basins, *J. Hydrol.*, 218, 1–12, doi:10.1016/S0022-1694(99)00011-6, <http://linkinghub.elsevier.com/retrieve/pii/S0022169499000116>, 1999.

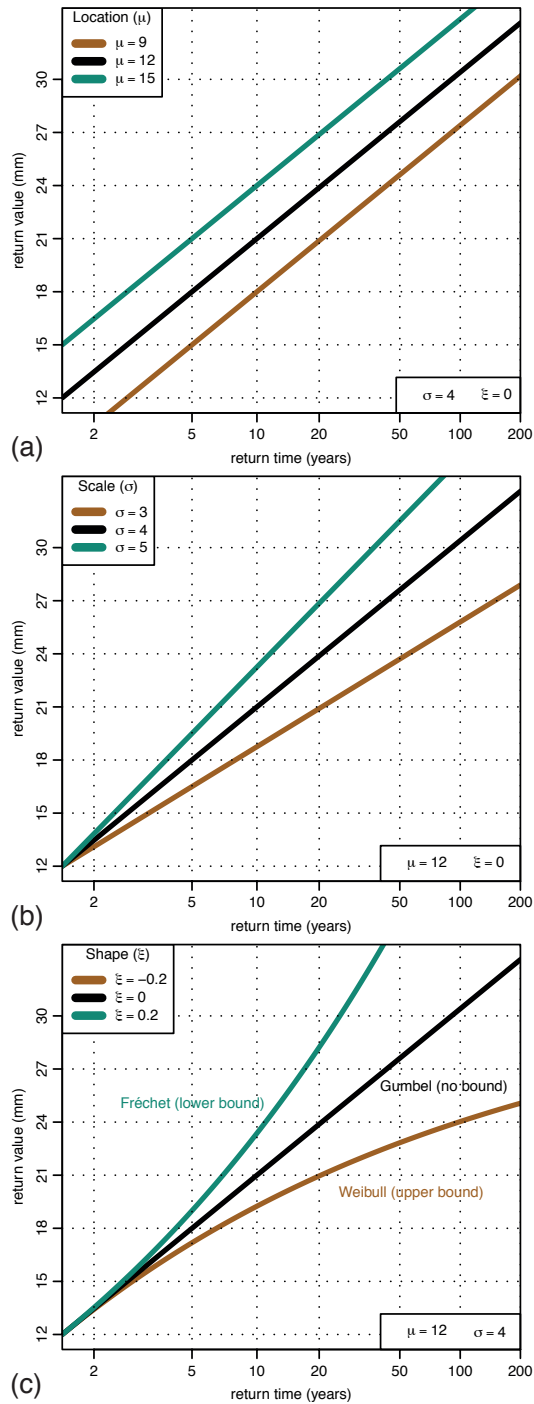


Figure S1. Illustration of GEV distribution parameters in a Gumbel diagram. (a) Varying the location parameter μ for constant σ and ξ , (b) varying the scale parameter σ for constant μ and ξ , and (c) varying the shape parameter ξ for constant μ and σ .

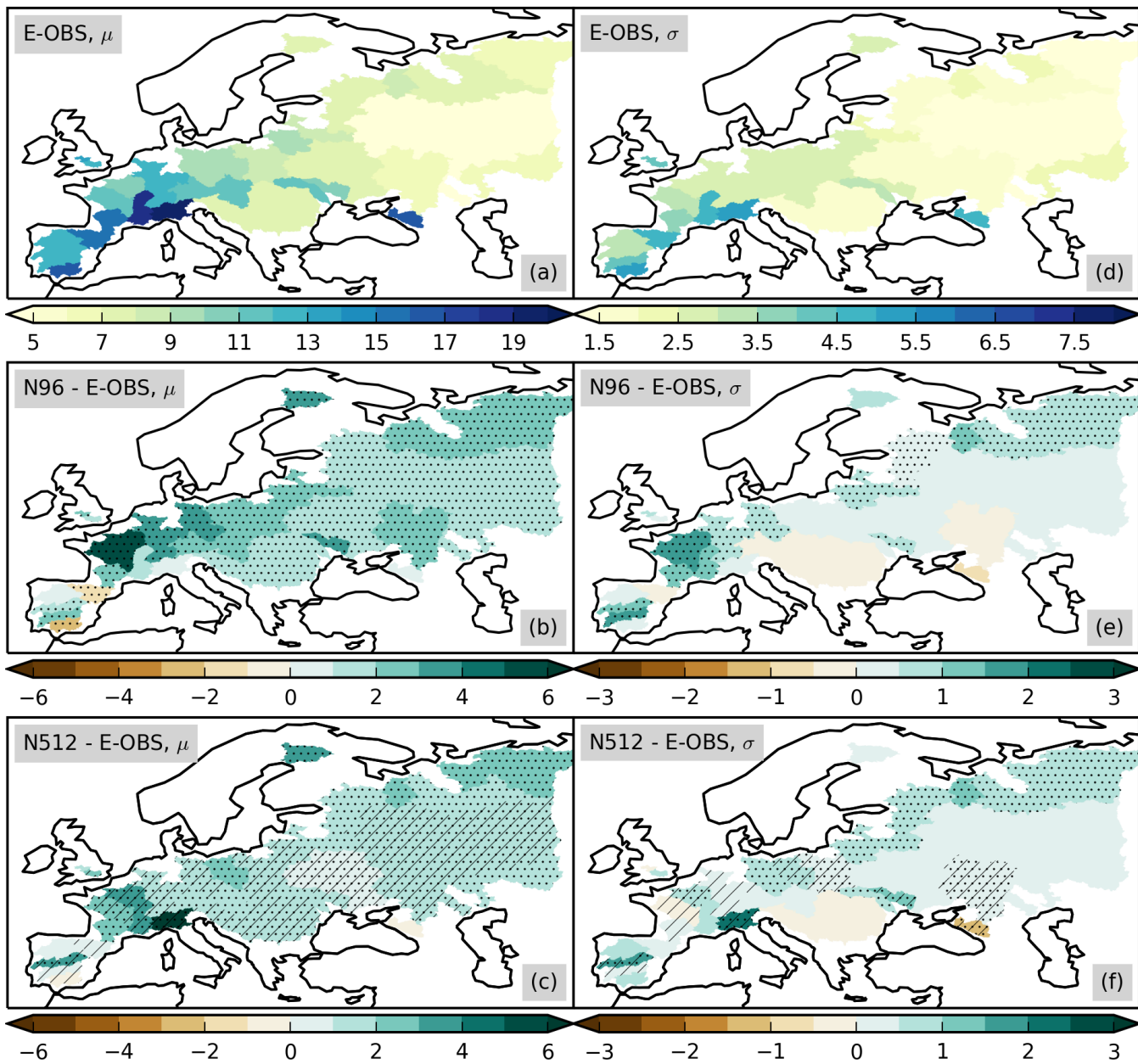


Figure S2. Estimated GEV parameters for March–May daily basin-average precipitation, (a–c) location parameter μ and (d–f) scale parameter σ , both in mm day^{-1} , and for (a,d) observations (E-OBS), (b,e) N96, and (c,f) N512 resolution. Stippling (hatching) shows statistically significant differences between the models and E-OBS (between N512 and N96).

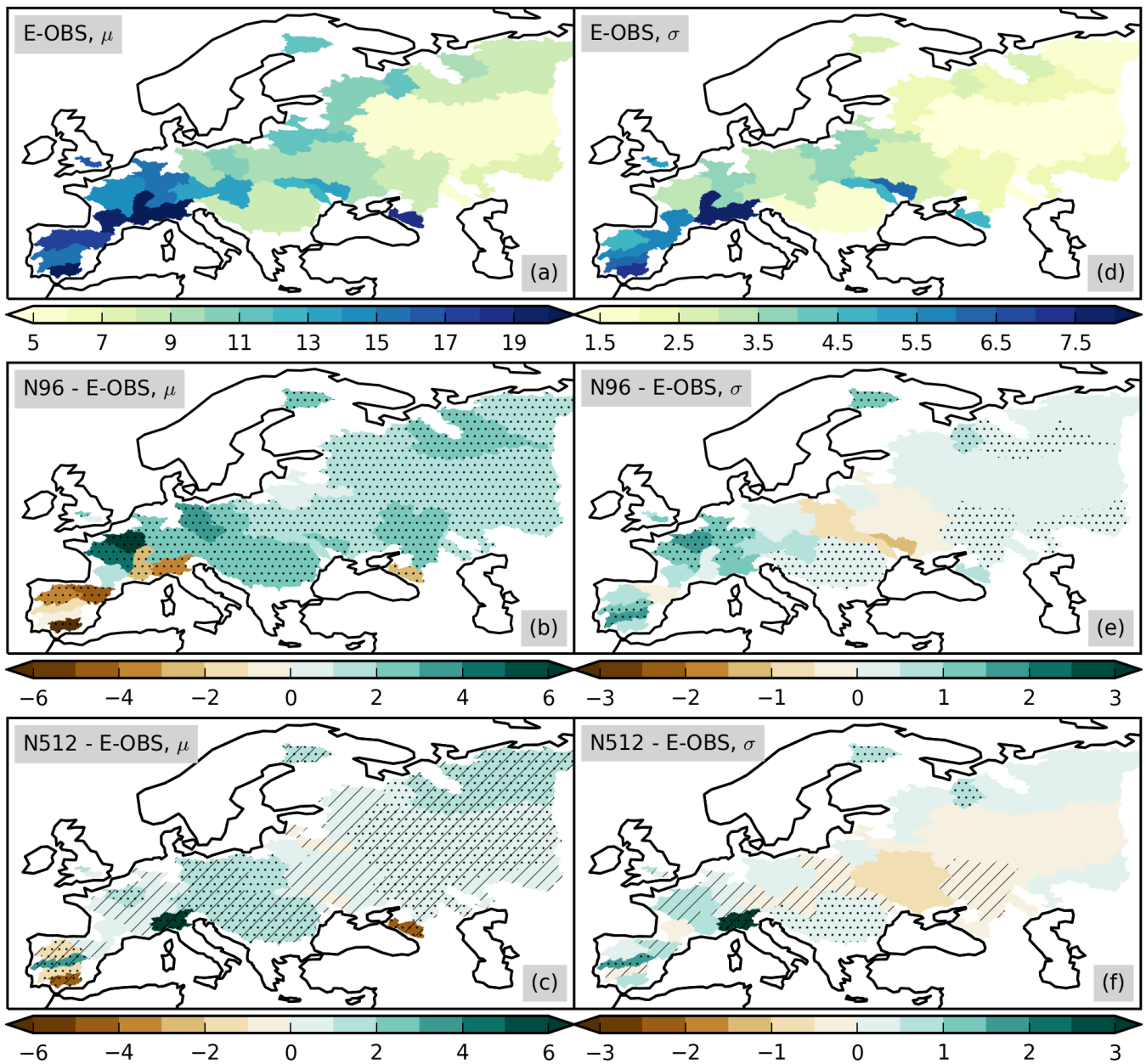


Figure S3. As Fig. S2 but for autumn (September–November).

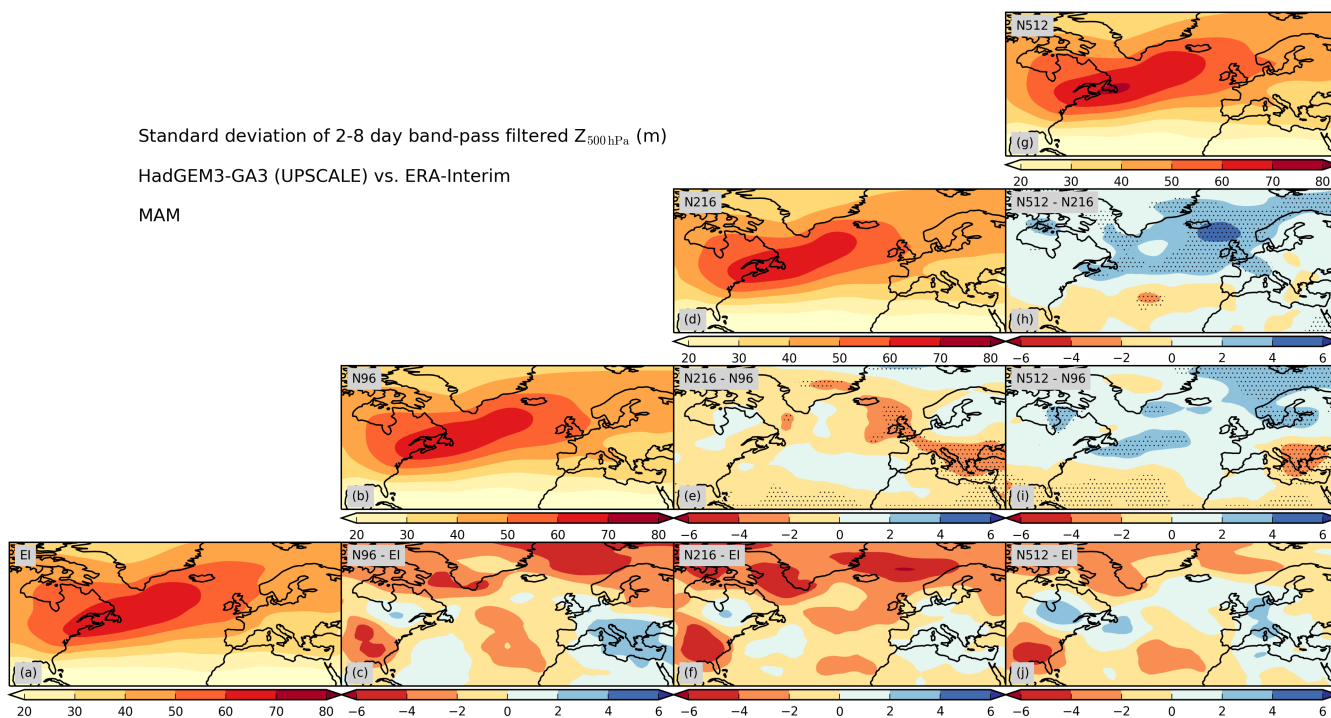


Figure S4. Standard deviation of 2–8 day band-pass filtered 500 hPa geopotential height (m) during spring (March–May). (a) ERA-Interim reanalysis, (b,d,g) model (HadGEM3-GA3.0) at resolutions N96, N216, and N512, (c,f,j) model biases with respect to E-OBS, and (e,h,i) differences between model resolutions. Stippling shows statistically significant differences.

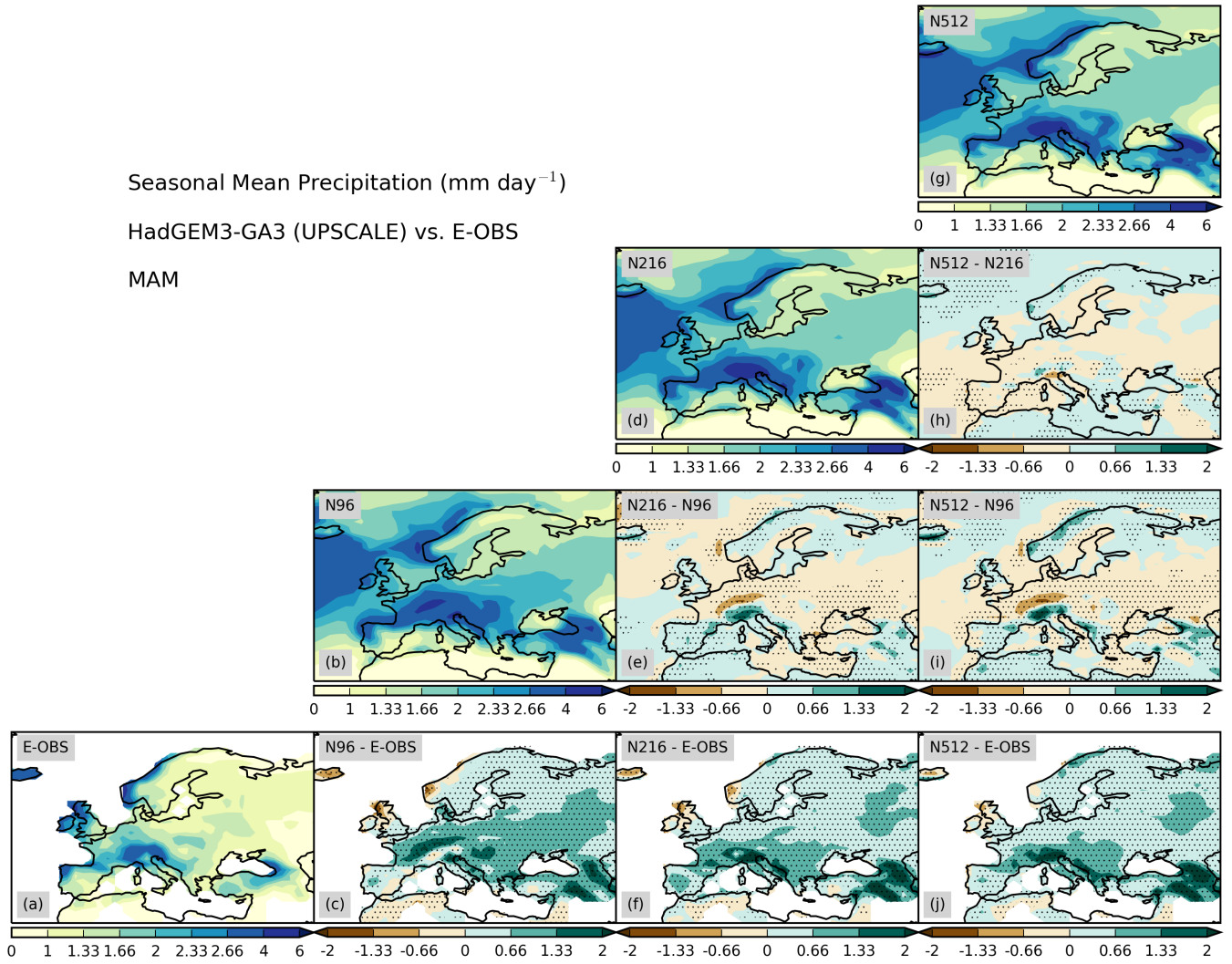


Figure S5. Spring (March–May) mean precipitation. (a) Observations (E-OBS), (b,d,g) model (HadGEM3-GA3.0) at resolutions N96, N216, and N512, (c,f,j) model biases with respect to E-OBS, and (e,h,i) differences between model resolutions. Stippling shows statistically significant differences.

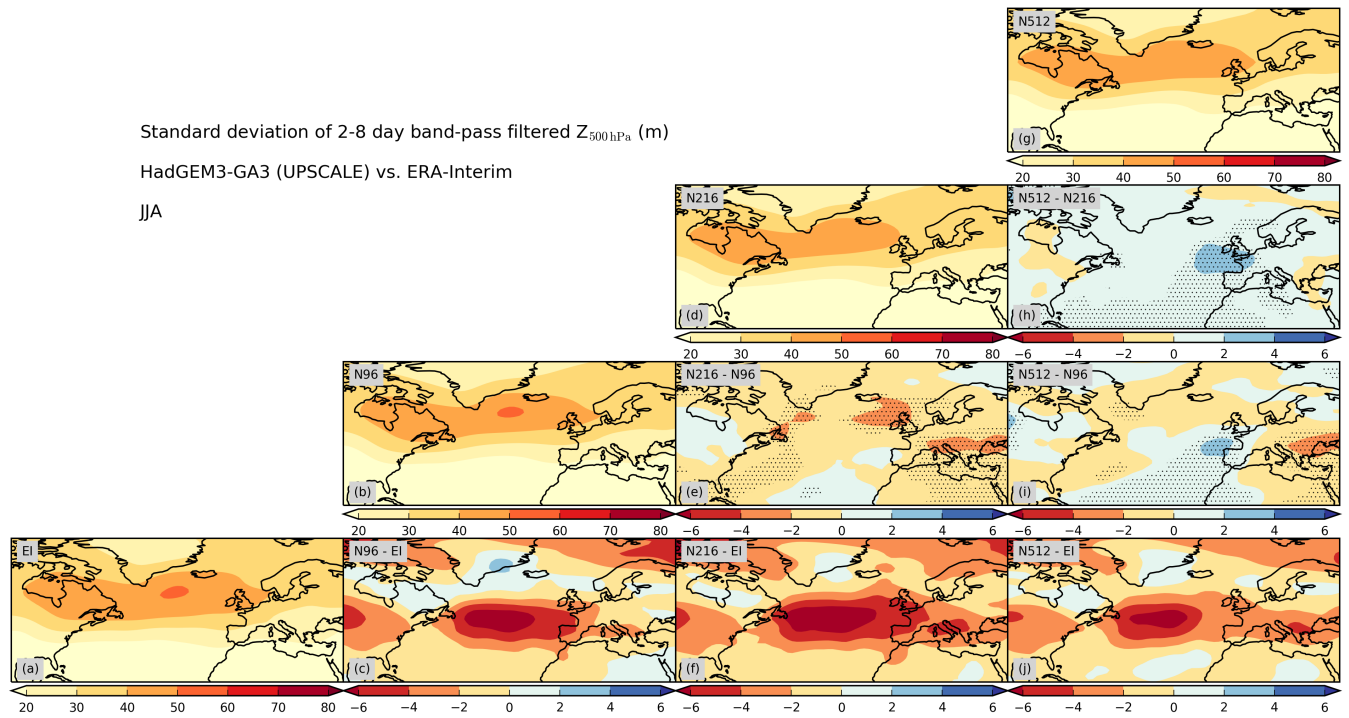


Figure S6. As Fig. S4 but for summer (June–August).

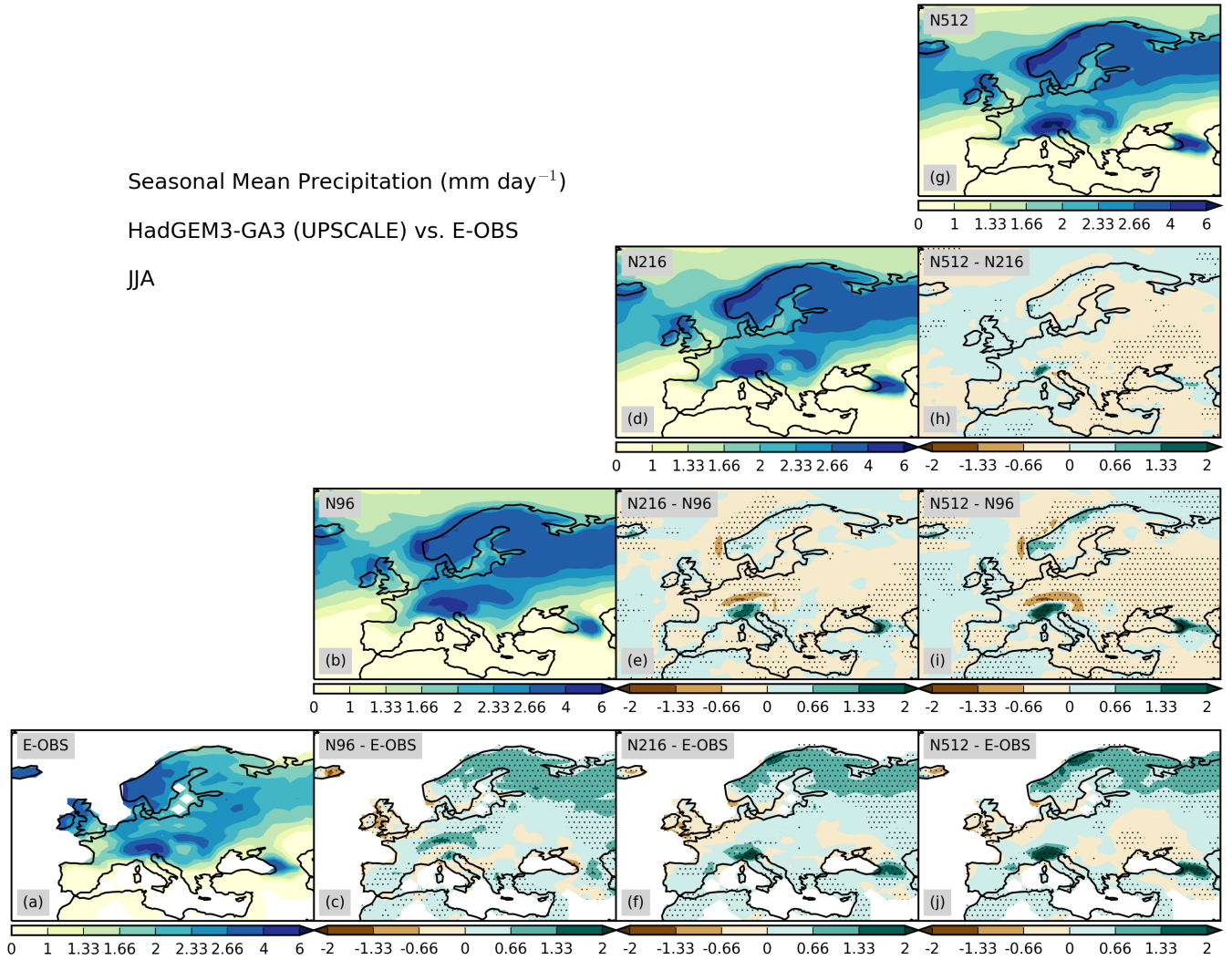


Figure S7. As Fig. S5 but for summer (June–August).

Standard deviation of 2-8 day band-pass filtered Z_{500hPa} (m)

HadGEM3-GA3 (UPSCALE) vs. ERA-Interim

SON

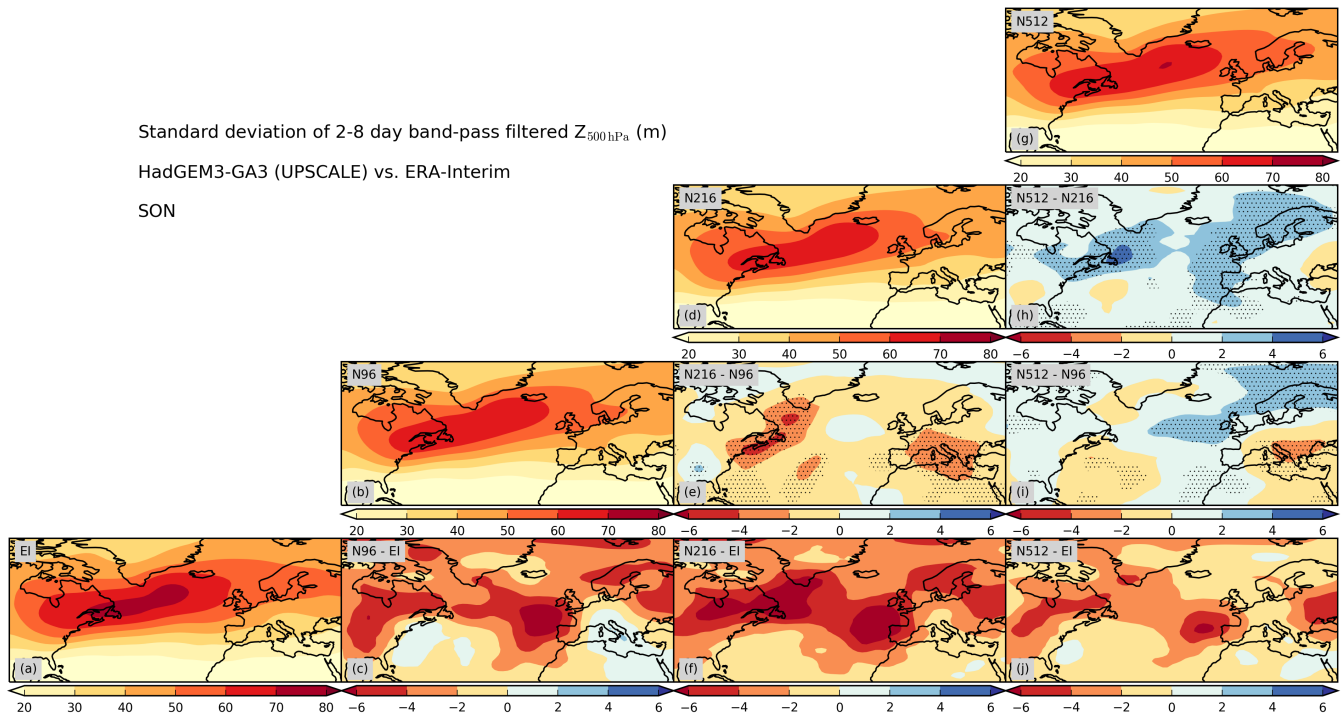


Figure S8. As Fig. S4 but for autumn (September–November).

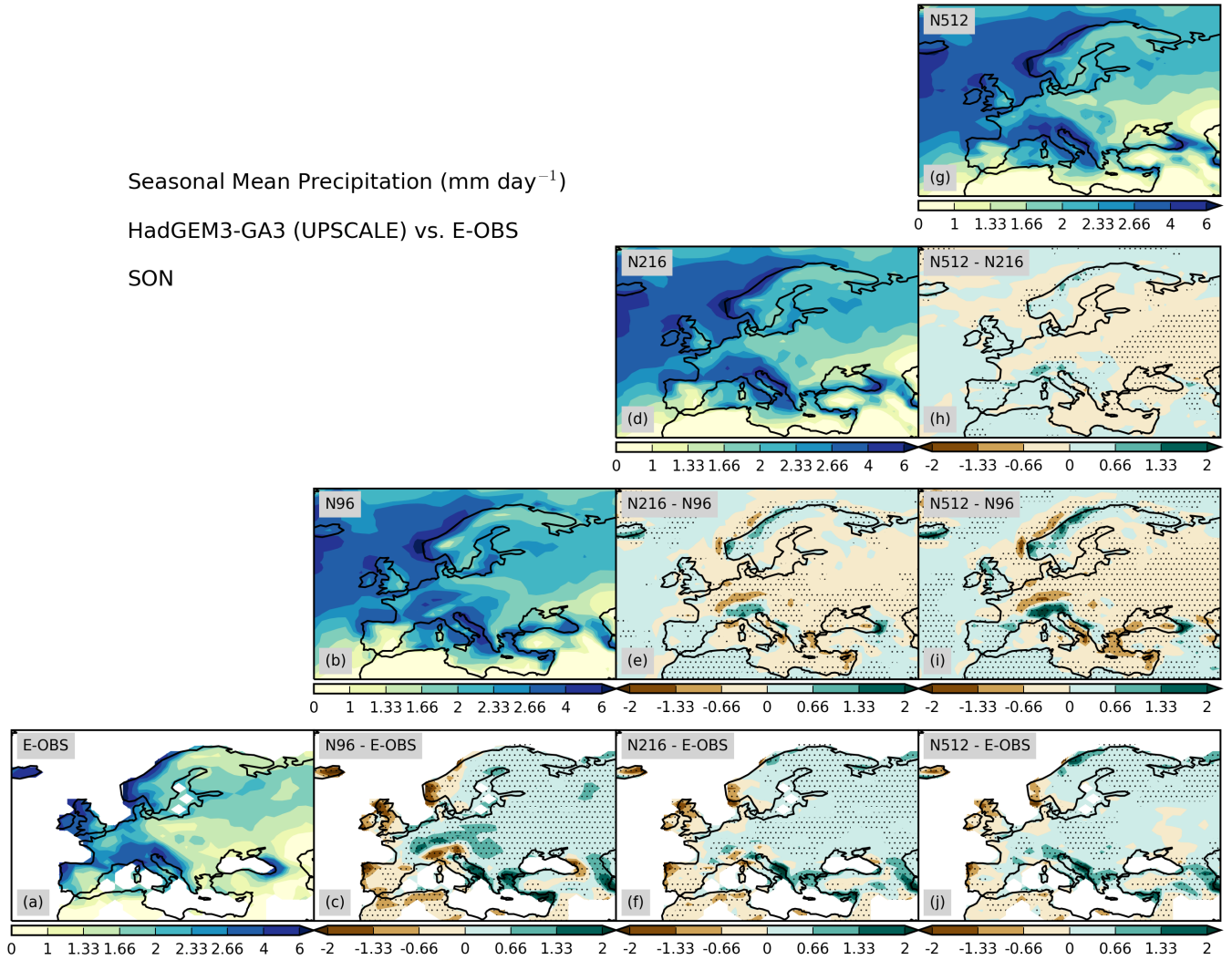


Figure S9. As Fig. S5 but for autumn (September–November).

Seasonal Mean Precipitation (mm day^{-1})

HadGEM3-GA6
N480 CTRL vs. N480 with N96 orography vs. E-OBS

MAM

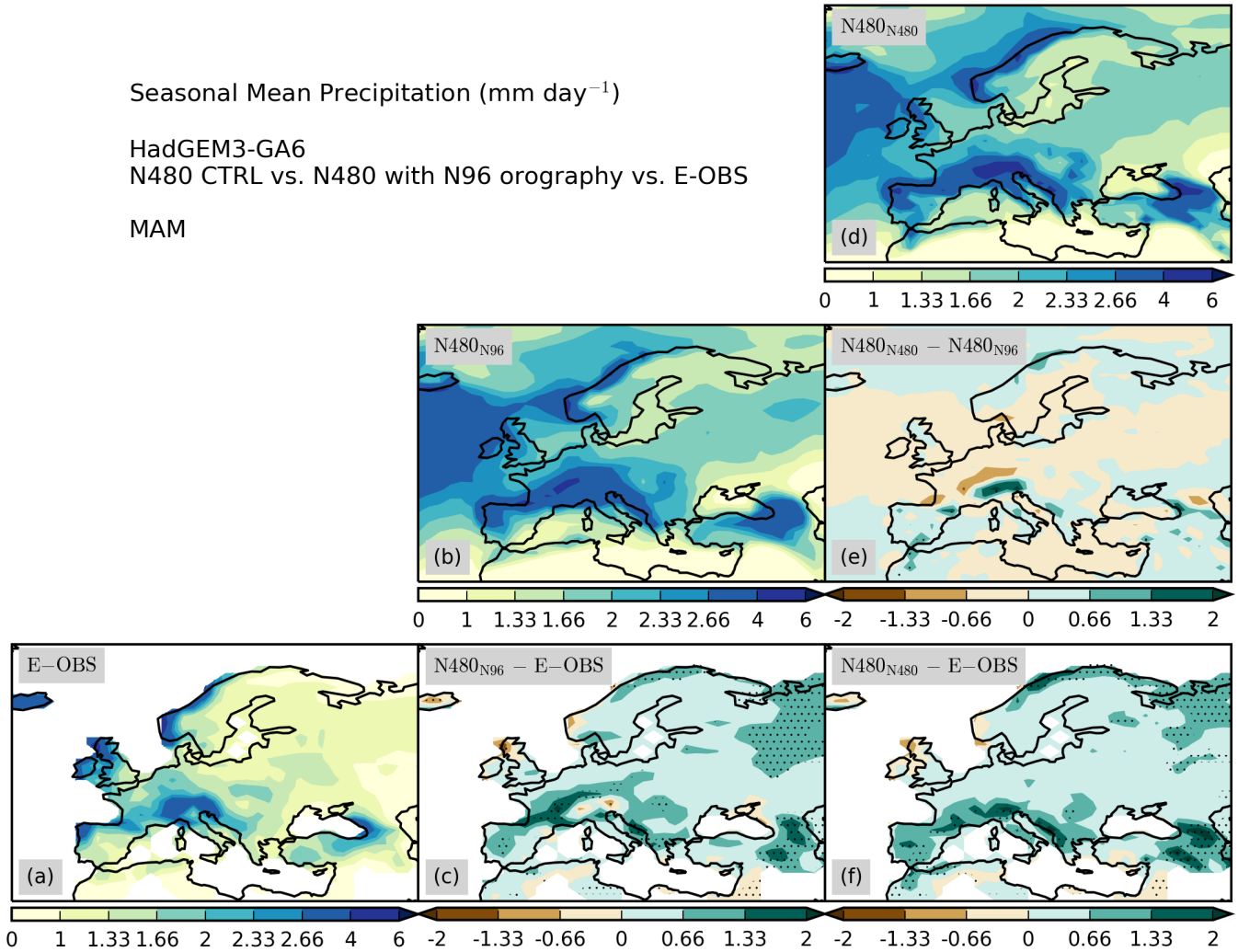


Figure S10. Spring (March–May) precipitation in mm day^{-1} in (a) observations (E-OBS), (b) the N480 model with N96 orography, and (d) the N480 control simulation. (c,f) Model bias with respect to E-OBS, (e) difference between the two model simulations. Stippling shows statistically significant differences.

Seasonal Mean Precipitation (mm day^{-1})

HadGEM3-GA6
N480 CTRL vs. N480 with N96 orography vs. E-OBS

JJA

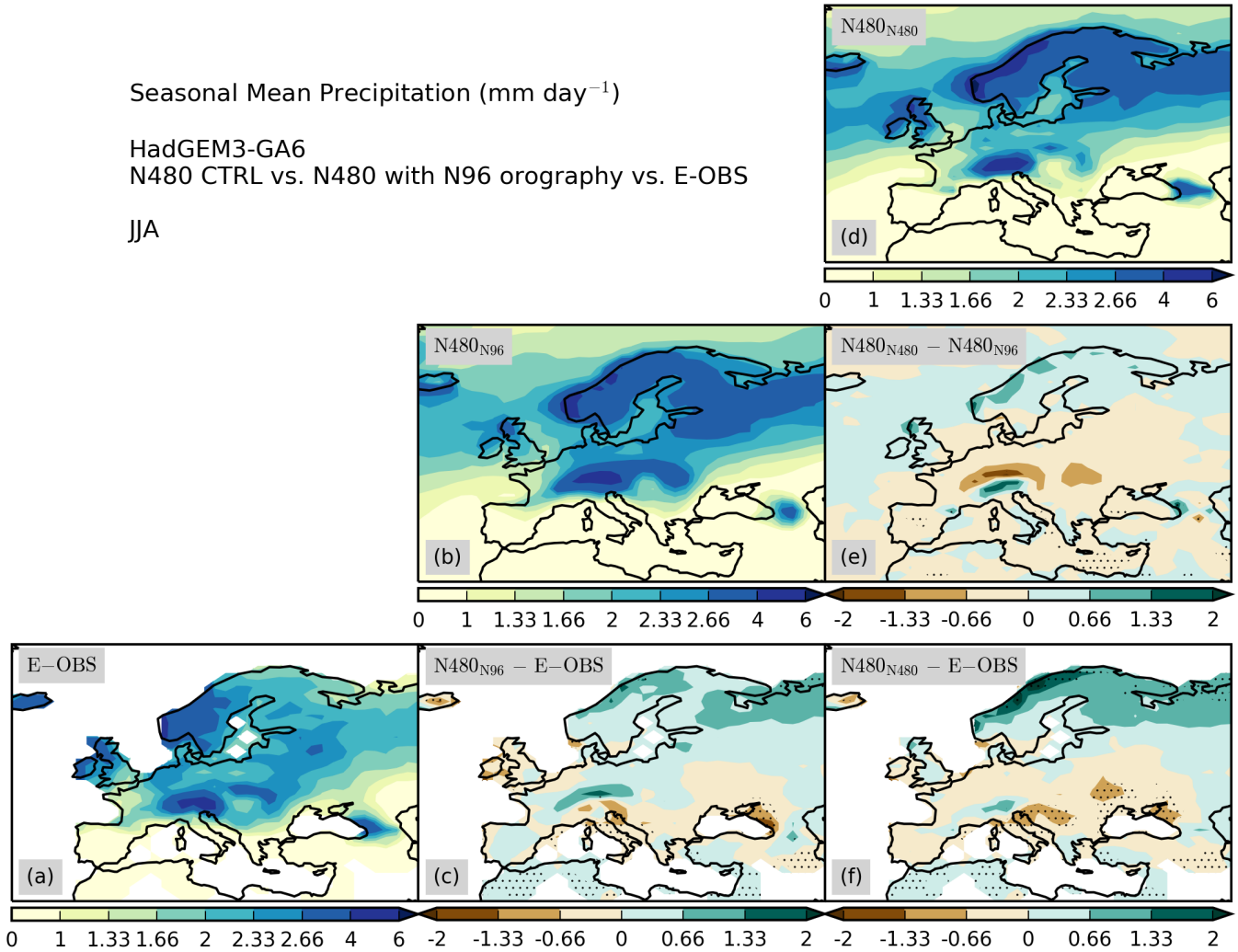


Figure S11. As Fig. S10 but for summer (June–August).

Seasonal Mean Precipitation (mm day^{-1})

HadGEM3-GA6

N480 CTRL vs. N480 with N96 orography vs. E-OBS

SON

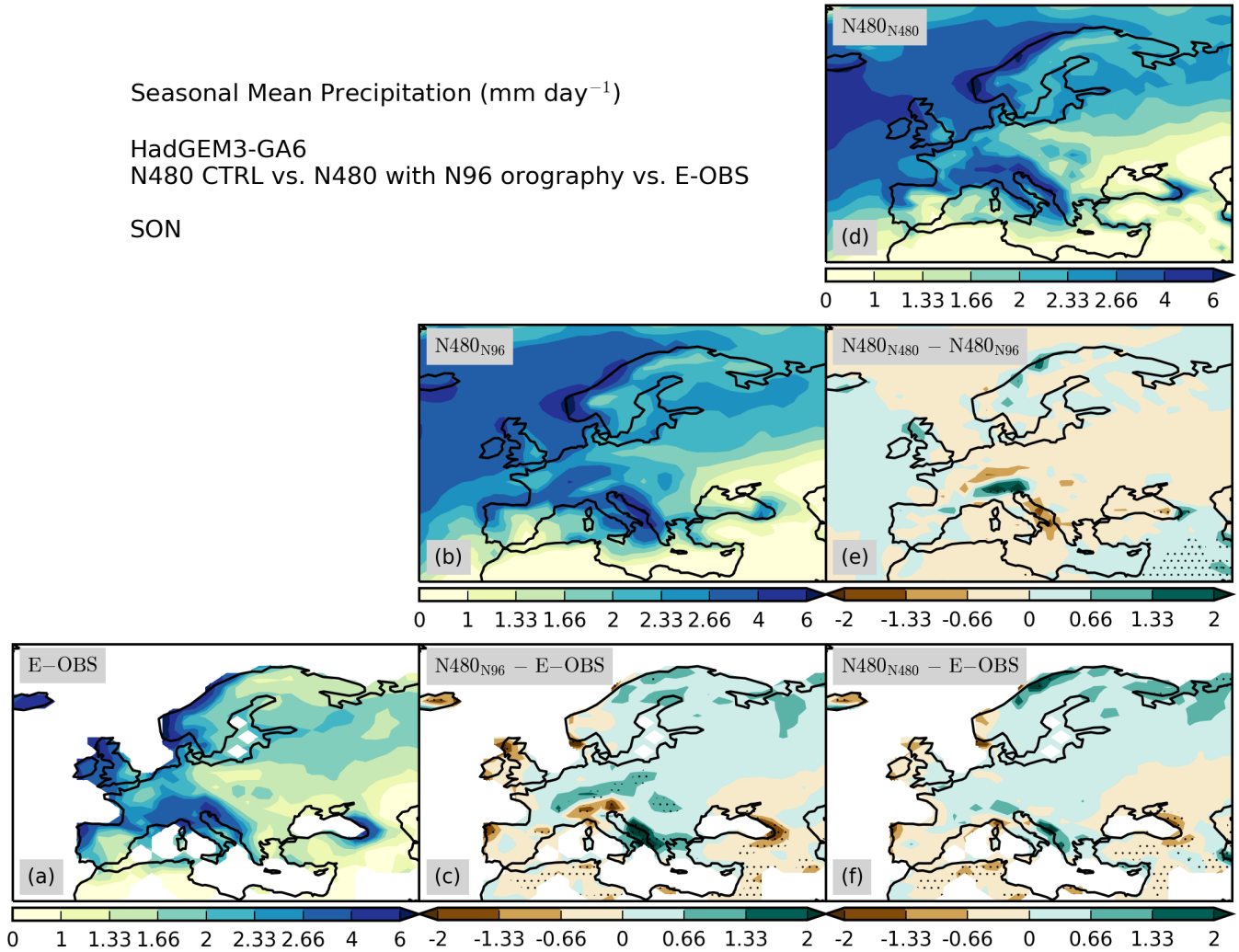


Figure S12. As Fig. S10 but for autumn (September–November).

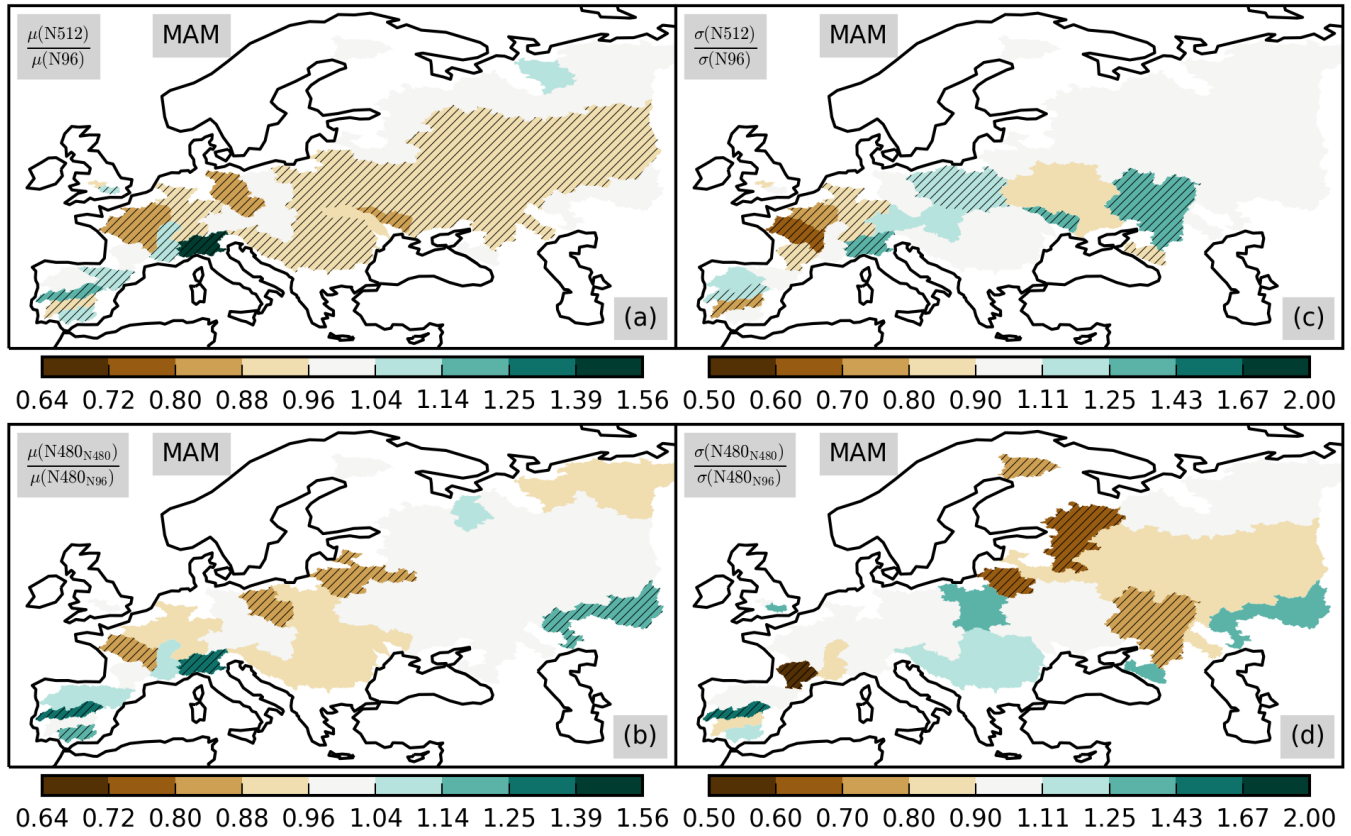


Figure S13. Spring (March–May) ratios of fitted GEV parameters for (a,b) the location parameter μ and for (c,d) the scale parameter σ , between (a,c) the N512 and N96 simulations and between (b,d) the N480 control simulation and the N480 simulation with N96 orography. Hatching shows statistically significant differences.

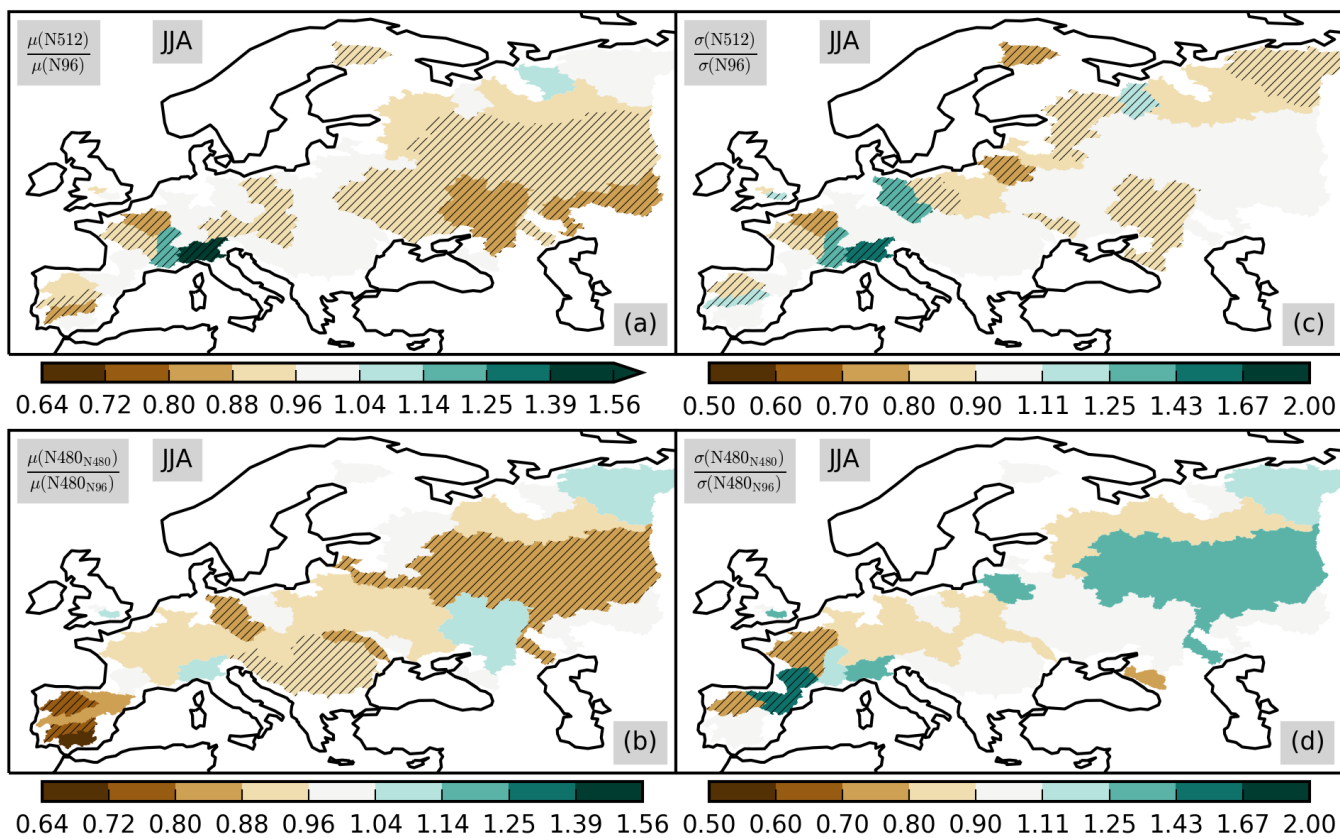


Figure S14. As Fig. S13 but for summer (June–August).

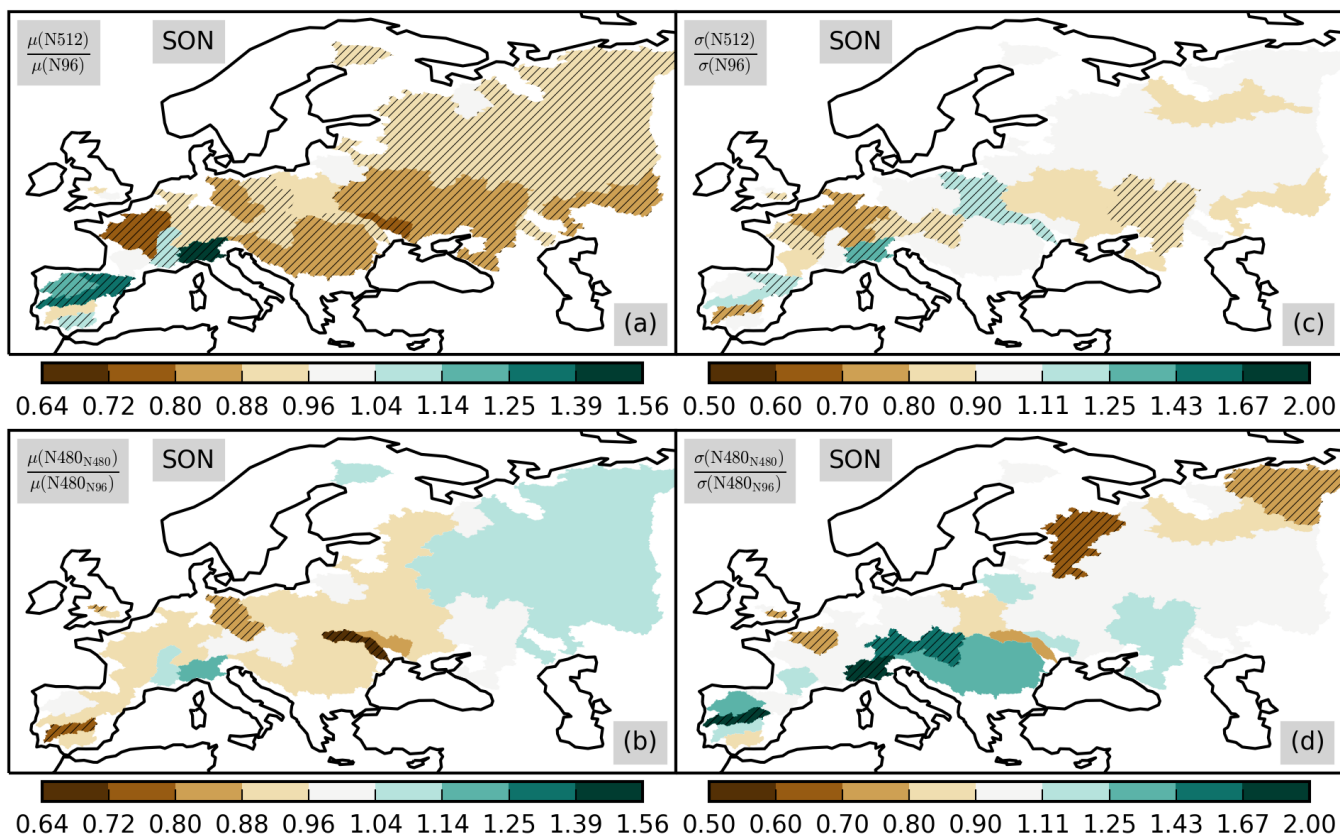


Figure S15. As Fig. S13 but for autumn (September–November).